PAIRUP-MS

Pathway analysis and imputation to relate unknowns in profiles from mass spectrometry-based metabolite data

Hsu, Yu-Han H.; Churchhouse, Claire; Pers, Tune H.; Mercader, Josep M.; Metspalu, Andres; Fischer, Krista; Fortney, Kristen; Morgen, Eric K.; Gonzalez, Clicerio; Gonzalez, Maria E.; Esko, Tonu; Hirschhorn, Joel N.

Published in:
PLOS Computational Biology

DOI:
10.1371/journal.pcbi.1006734

Publication date:
2019

Document version
Publisher's PDF, also known as Version of record

PLOS COMPUTATIONAL BIOLOGY

RESEARCH ARTICLE

PAIRUP-MS: Pathway analysis and imputation to relate unknowns in profiles from mass spectrometry-based metabolite data

Yu-Han H. Hsu[1,2,3], Claire Churchhouse[4,5], Tune H. Pers[6,7], Josep M. Mercader[3,8], Andres Metspalu[9], Krista Fischer[9,10], Kristen Fortney[11], Eric K. Morgen[11], Clicerio Gonzalez[12,13], Maria E. Gonzalez[12,13], Tonu Esko[3,9], Joel N. Hirschhorn[1,2,3]*

1 Department of Genetics, Harvard Medical School, Boston, Massachusetts, United States of America, **2** Division of Endocrinology and Center for Basic and Translational Obesity Research, Boston Children's Hospital, Boston, Massachusetts, United States of America, **3** Programs in Metabolism and Medical & Population Genetics, Broad Institute of Harvard and MIT, Cambridge, Massachusetts, United States of America, **4** Stanley Center for Psychiatric Research, Broad Institute of Harvard and MIT, Cambridge, Massachusetts, United States of America, **5** Analytical and Translational Genomics Unit, Massachusetts General Hospital, Boston, Massachusetts, United States of America, **6** Novo Nordisk Foundation Centre for Basic Metabolic Research, University of Copenhagen, Copenhagen, Denmark, **7** Department of Epidemiology Research, Statens Serum Institut, Copenhagen, Denmark, **8** Diabetes Unit and Center for Genomic Medicine, Massachusetts General Hospital, Boston, Massachusetts, United States of America, **9** Estonian Genome Center, Institute of Genomics, University of Tartu, Tartu, Estonia, **10** Institute of Mathematics and Statistics, University of Tartu, Tartu, Estonia, **11** BioAge Labs, Richmond, CA, United States of America, **12** Instituto Nacional de Salud Publica, Cuernavaca, Morelos, Mexico, **13** Centro de Estudios en Diabetes, Mexico City, Mexico

* Joel.Hirschhorn@childrens.harvard.edu

Citation: Hsu Y-HH, Churchhouse C, Pers TH, Mercader JM, Metspalu A, Fischer K, et al. (2019) PAIRUP-MS: Pathway analysis and imputation to relate unknowns in profiles from mass spectrometry-based metabolite data. PLoS Comput Biol 15(1): e1006734. https://doi.org/10.1371/journal.pcbi.1006734

Editor: Oliver Kohlbacher, University of Tuebingen, GERMANY

Received: January 25, 2018

Accepted: December 23, 2018

Published: January 14, 2019

Data Availability Statement: PAIRUP-MS source code and documentation are available on GitHub (https://github.com/yuhanhsu/PAIRUP-MS). Individual-level metabolite data for the OE cohort and the signal-metabolite set annotation matrix constructed from BioAge data are also available on the GitHub. Due to Estonian Biobank's regulations, individual-level OE genetic data and BioAge data need to be requested through an application to the biobank (https://www.geenivaramu.ee/en/biobank.ee/data-access). Other questions about OE and

Abstract

Metabolomics is a powerful approach for discovering biomarkers and for characterizing the biochemical consequences of genetic variation. While untargeted metabolite profiling can measure thousands of signals in a single experiment, many biologically meaningful signals cannot be readily identified as known metabolites nor compared across datasets, making it difficult to infer biology and to conduct well-powered meta-analyses across studies. To overcome these challenges, we developed a suite of computational methods, PAIRUP-MS, to match metabolite signals across mass spectrometry-based profiling datasets and to generate metabolic pathway annotations for these signals. To pair up signals measured in different datasets, where retention times (RT) are often not comparable or even available, we implemented an imputation-based approach that only requires mass-to-charge ratios (m/z). As validation, we treated each shared known metabolite as an unmatched signal and showed that PAIRUP-MS correctly matched 70–88% of these metabolites from among thousands of signals, equaling or outperforming a standard m/z- and RT-based approach. We performed further validation using genetic data: the most stringent set of matched signals and shared knowns showed comparable consistency of genetic associations across datasets. Next, we developed a pathway reconstitution method to annotate unknown signals using curated metabolic pathways containing known metabolites. We performed genetic validation for the generated annotations, showing that annotated signals associated with gene variants were more likely to be enriched for pathways functionally related to the genes

BioAge data access should be directed to co-author Tonu Esko (tesko@broadinstitute.org). We do not have ownership of the MCDS data and obtained permission to analyze the data from the SIGMA T2D Consortium. Previously published MCDS data can be accessed through the T2D Knowledge Portal (http://www.type2diabetesgenetics.org) and inquiries for unpublished data should be directed to Jose Florez (jcflorez@mgh.harvard.edu) and Dorothy Pazin (dorothy@broadinstitute.org).

Funding: This work was supported by the National Heart, Lung, and Blood Institute (https://www.nhlbi.nih.gov) grant F31HL126581 (Y.H.H.), National Institute of Diabetes and Digestive and Kidney Diseases (https://www.niddk.nih.gov) grant R01DK075787 (J.N.H.), Doris Duke Charitable Foundation (http://www.ddcf.org) grant 215205 (J. N.H.), Estonian Research Council (http://www.etag.ee/en/estonian-research-council/) grants IUT20-60 (A.M.), PUT1665 (K.Fischer), PUT1660 (T.E.), European Union through Horizon 2020 (https://ec.europa.eu/programmes/horizon2020/) grant 692145 (A.M.), European Union through the European Regional Development Fund (http://ec.europa.eu/regional_policy/en/funding/erdf/) Project No. 2014-2020.4.01.15-0012 (A.M.), and Lundbeck Foundation (https://www.lundbeckfonden.com/en/) grant R190-2014-3904 (T.H.P.). The funders had no role in study design, data collection and analysis, decision to publish, or preparation of the manuscript.

Competing interests: I have read the journal's policy and the authors of this manuscript have the following competing interests: K.Fortney and E.K. M. are affiliated with BioAge Labs, Inc.; J.N.H. serves on the Scientific Advisory Board of Camp4 Therapeutics.

compared to random expectation. Finally, we applied PAIRUP-MS to study associations between metabolites and genetic variants or body mass index (BMI) across multiple datasets, identifying up to ~6 times more significant signals and many more BMI-associated pathways compared to the standard practice of only analyzing known metabolites. These results demonstrate that PAIRUP-MS enables analysis of unknown signals in a robust, biologically meaningful manner and provides a path to more comprehensive, well-powered studies of untargeted metabolomics data.

Author summary

Untargeted metabolomics can systematically profile thousands of metabolite signals in biological samples and is an increasingly popular approach for discovering biomarkers and predictors for human traits and diseases. However, currently, a significant portion of the measured signals cannot be identified as known metabolites or easily compared across datasets, and thus are usually excluded from downstream analyses. Here, we present PAIRUP-MS, a suite of computational methods designed to analyze unknown, unidentified signals across multiple mass spectrometry-based profiling datasets. Specifically, PAIRUP-MS contains a flexible imputation-based approach for pairing up unknown signals across datasets, allowing for meta-analysis of matched signals across studies that would otherwise be incompatible. PAIRUP-MS also offers a pathway annotation and enrichment analysis framework that links metabolite signals to plausible biological functions without using their chemical identities. Importantly, we validated both components of PAIRUP-MS using genetic data and applied them to study an example trait, body mass index. Overall, our results demonstrate that PAIRUP-MS enables previously infeasible analyses of unknown, unidentified signals across multiple datasets, thereby greatly improving power for discovery and biological inference.

Introduction

Metabolomics is a powerful systematic approach for studying circulating molecules in biological samples [1, 2]. Profiling technologies such as nuclear magnetic resonance (NMR) spectroscopy and liquid or gas chromatography followed by mass spectrometry (LC-MS or GC-MS) have been used to discover metabolites that are biomarkers or predictors for various human traits and diseases, including clinical risk factors of metabolic or cardiovascular diseases [3], type 2 diabetes [4], and all-cause mortality [5]. Genome-wide association studies (GWAS) have also identified numerous metabolic quantitative trait loci (mQTLs) that influence variation in metabolite abundance, which may provide valuable insights into gene functions and disease mechanisms [6–9].

While metabolomics has led to many new discoveries, a significant portion of the generated data have not been used to its full potential. Untargeted profiling platforms collect measurements for thousands of metabolite signals and compare their data to standards in compound databases to identify known metabolites [1]. Current identification procedures can identify up to a few hundred known metabolites and the remaining unknown signals are often excluded from downstream analyses. However, studying unknown signals may be fruitful for several reasons. First, many unknowns show correlation with known metabolites, phenotypes, and genetic variants, indicating that they capture biological information [10]. Second, because

unknowns usually make up a large portion of untargeted data, including them can greatly increase the search space in analyses. Finally, investigating unknown signals may enable us to discover novel biomarkers that have not been characterized in human metabolism. Therefore, developing computational methods that deal with unknown signals is critical for making the most out of untargeted metabolomics data.

Analyzing unknown signals poses several challenges. Distinguishing biological signals from noise and adjusting for technical artifacts are difficult, because unknowns are often associated with noisier measurements compared to known metabolites [11]. Meta-analysis, which may increase power for detecting noisy but true signals, is complicated by the lack of gold standard protocols and varying signal characteristics across platforms and studies. While some methods have been developed to align signals across datasets using mass-to-charge ratio (m/z) and/or retention time (RT) information, their applications are often restricted to processing data batches within a single study or data generated by the same profiling method [11–13]. Another main challenge is to link unknown signals to biological functions before confirming their exact chemical identities. Although several pathway or network-based approaches have incorporated unknown signals into metabolomics analyses, they focus on a small subset of the unknowns (e.g. those directly associated with known metabolites, genes, or a trait of interest) and do not explicitly provide biological interpretations (e.g. pathway labels) for enriched pathways or network clusters identified during analysis [10, 14, 15].

To overcome the challenges described above, we developed and implemented a suite of computational methods, PAIRUP-MS (Pathway Analysis and Imputation to Relate Unknowns in Profiles from MS-based metabolite data), for analyzing unknown signals. PAIRUP-MS can be applied to MS-based profiling datasets in which signal peaks have been detected, aligned, and quantified, and where some peaks have been identified as known metabolites. PAIRUP-MS is used to further process, match, and annotate the unknown signals and to perform meta-analysis and pathway-based analysis that include unknown signals. We utilized genetic associations to validate the methods and demonstrated their application by studying metabolite signals associated with body mass index (BMI). Our framework can be applied to diverse untargeted profiling datasets produced by typical MS-based profiling platforms and will help to advance metabolomics as a powerful approach for elucidating biology underlying human traits and diseases.

Results

Metabolomics datasets and data processing

We developed and tested PAIRUP-MS using LC-MS profiling data generated from three independent cohorts: (1) Obesity Extremes cohort (OE): 300 individuals (100 lean, 100 obese, and 100 population control) sampled from the Estonian Biobank, (2) Mexico City Diabetes Study cohort (MCDS): 865 individuals in a prospective type 2 diabetes study, and (3) BioAge Labs Mortality cohort (BioAge): 583 individuals selected from the Estonian Biobank for a retrospective mortality study. In order to reduce noise in the profiling data and to improve power in analyses, we implemented a quality control (QC) pipeline to adjust each dataset for measurement variation associated with technical artifacts and remove samples, metabolite signals, and data points with noisy trends (**S1 Fig**). After QC, we leveraged the correlation structure among signals to impute any remaining missing values within a dataset. In the end, the OE dataset contained 298 samples and 13,613 metabolite signals (322 known and 13,291 unknown); MCDS contained 821 samples and 7,136 signals (242 known and 6,894 unknown); BioAge contained 583 samples and 14,617 signals (603 known and 14,014 unknown). Covariate adjustment (if appropriate) and rank-based inverse normal transformation were performed on each

Table 1. Characteristics of study cohorts and corresponding metabolomics datasets.

	Obesity Extremes cohort (OE)	Mexico City Diabetes Study cohort (MCDS)	BioAge Labs Mortality cohort (BioAge)
Study design	BMI extremes from Estonian Biobank (EB)	Prospective cohort for type 2 diabetes	Retrospective cohort for mortality from EB
# of samples	298	821	583
# of women (%)	149 (50.0)	498 (60.7)	407 (69.8)
Age (yr)	38.5 ± 12.1	52.3 ± 7.73	73.3 ± 2.70
BMI (kg/m^2)	28.3 ± 9.95	28.6 ± 4.54	27.3 ± 4.33
Fasting time* **(hr)**	7.42 ± 3.34	overnight	3.04 ± 2.80
Profiling methods**	*C8-pos*, *C18-neg*, *HILIC-pos*, HILIC-neg	*LIPID*, *HILIC-pos*, CMH	*C8-pos*, *C18-neg*, *HILIC-pos*, *HILIC-neg*
# of signals (# of knowns)	13,613 (322)	7,136 (242)	14,617 (603)
# of signals with m/z data (# of knowns)	13,552 (261)	7,083 (189)	14,617 (603)

Mean ± standard deviation is reported for quantitative phenotypes.

* Fasting time for OE and BioAge was not exact due to conversion from categorical variable; 200 BioAge samples had no fasting time information.

** Italicized profiling methods had m/z and RT information available; we treated "C8-pos" and "LIPID" to be the same method in our analyses due to large overlap in the metabolites they measured; see S1 Text for profiling method details.

https://doi.org/10.1371/journal.pcbi.1006734.t001

metabolite signal and the resulting abundance *z*-scores were used in downstream analyses. QC'ed cohort and dataset characteristics are summarized in Table 1. Known metabolites in QC'ed datasets are listed in S1 Table.

Matching metabolite signals across datasets

Matching method overview. An approach for comparing unknown signals measured in different untargeted profiling datasets is crucial for increasing power in metabolomics studies. Instead of using RT information, which can vary greatly across profiling methods and platforms, we developed a method that utilizes m/z and imputation to match up signals likely to represent the same metabolites across MS-based profiling datasets (Fig 1A). In preliminary analysis, we observed that known metabolites measured across our three datasets had moderately similar correlation structures despite substantial differences in study populations and designs (S2 Fig). We took advantage of this observation and imputed the abundance of unknown (or unshared known) signals from one dataset to another using shared known metabolites as predictors in linear regression models. The imputation then allowed us to calculate the correlation between signals measured in different datasets across a common set of samples and to pair up signals based on agreement in m/z and this correlation.

Calibration using shared known metabolites. In order to calibrate parameters in our method, we treated known metabolites shared across two datasets as unmatched signals and applied our method to match each of them in turn. We compared the performance of different parameter settings by calculating the percentage of matches that were either the correct match or highly correlated ($r^2 > 0.8$) with the correct match in observed data. The parameter choices we tested included: (1) whether to consider different adduct ions when checking for m/z agreement, (2) which set of samples to use for calculating correlation between signals, (3) whether to allow multiple-to-1 signal matching or require unique 1-to-1 matching, (4) whether to match only signals measured by the same profiling method or allow matching across different methods, and, optionally, (5) which correlation cutoff threshold to use for calling a match.

The calibration results for OE-MCDS, OE-BioAge, and MCDS-BioAge matching are shown in S3–S5 **Figs** and the optimal parameter settings chosen for each dataset pair are

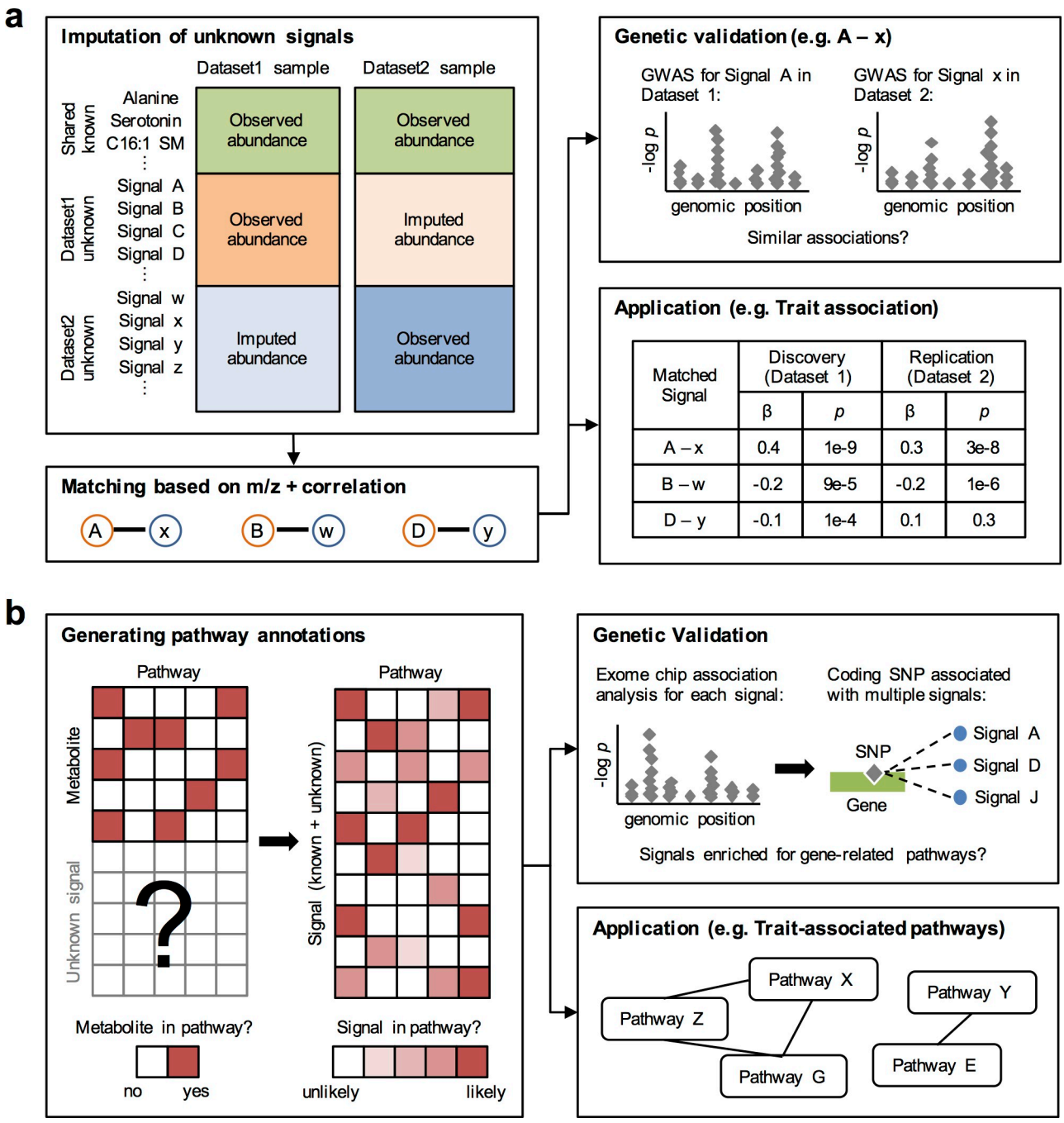

Fig 1. PAIRUP-MS is a suite of computational methods for analyzing metabolite signals in untargeted metabolomics data. (a) Overview of matching method: unknown (or unshared known) signals are imputed across datasets using shared known metabolites as predictors and then paired up based on m/z and correlation across samples. Genetic data can be used to validate matched signal pairs that share similar genetic associations. Matched signals can be used to perform combined association analyses across datasets (e.g. identifying trait-associated signals in discovery and replication cohorts). (b) Overview of pathway method: using binary metabolic pathway annotations and untargeted profiling data as input, a pathway reconstitution procedure is performed to construct a numeric annotation matrix, where each signal (known or unknown) gets a membership score in each pathway (or "metabolite set", see Methods). Genetic data can be used to validate that signals associated with a specific gene are enriched for reconstituted pathways related to the gene. The annotation matrix can be used to perform pathway analyses (e.g. identifying pathways enriched for a list of trait-associated signals).

https://doi.org/10.1371/journal.pcbi.1006734.g001

summarized in S2A Table. We decided to consider two types of matches, "multiple" and "reciprocal", for subsequent analyses. Briefly, in the "multiple" setting, we matched each Dataset 1 signal, *s*, to a Dataset 2 signal by first identifying all Dataset 2 signals whose m/z agree with *s*, and then selecting the one that has the best correlation with *s* to be the final match. Following this procedure, more than one Dataset 1 signal may be mapped to the same Dataset 2 signal. For "reciprocal" matches, we repeated the same procedure to match Dataset 1 signals to Dataset 2 and vice versa, and only kept the subset of matches that were generated in both directions. Our method performed slightly better using the "reciprocal" setting, in which it correctly paired up 69.9 to 87.6% of the matched knowns, with 91.6 to 96.4% of all matches showing strong correlation ($r^2 > 0.8$) with the correct match. However, the "multiple" setting also performed relatively well (58.4 to 87.1% of matches were correct; 91.0 to 96.1% were highly correlated) and identified more correct or highly correlated matches overall, so both match types can be useful, depending on the analysis context.

We compared our method against a m/z and RT-based matching approach, where signals with agreeing m/z were mapped to each other based on predicted RT calculated from shared known metabolite data. The imputation method generally performed as well as or slightly better than the RT method, despite not using any RT information (S2A Table). An important advantage of the imputation approach is that, even when the matches made for known metabolites were incorrect, ~60–80% of them were strongly correlated ($r^2 > 0.8$) with the true known matches. In contrast, incorrect matches made by the RT approach sometimes showed much weaker correlation. These results suggest that our method can be used to discover "proxies" for metabolites in a dataset even when an exact match does not exist or could not be identified. Furthermore, when we allowed matching across profiling methods, the RT approach showed a bigger dip in performance compared to the imputation approach (S2B Table). Thus, imputation-based matching may be a more flexible framework for comparing datasets generated by diverse profiling platforms, especially when directly comparable RT data is not available.

Dataset characteristics such as sample size, number of shared known metabolites, and similarity in metabolite correlation structure can influence performance of the imputation-based matching approach. We ran additional analyses using random subsets of MCDS and BioAge samples to assess matching performance across a range of sample sizes (S6A Fig). We observed that the fraction of correct or highly correlated matched knowns tended to increase with sample size, stabilizing after each dataset contained at least ~300 samples. Similarly, when we performed matching using subsets of MCDS-BioAge shared known metabolites as predictors during imputation, performance improved as the number of shared knowns increased (S6B Fig). Finally, to check how overall similarity in metabolite correlation structure influences matching performance, we assessed OE-MCDS, OE-BioAge, and MCDS-BioAge similarities by first calculating pairwise correlations between shared known metabolites within each dataset and then calculating the correlation of these pairwise correlations across each pair of datasets (S2 Fig). We observed that the most similar dataset pair, MCDS-BioAge ($r^2 = 0.625$), had the best matching performance, while the least similar pair, OE-MCDS ($r^2 = 0.400$), performed the worst (S2A Table). Together, these results indicate that the imputation-based matching procedure is more effective at matching larger datasets with more known metabolites and composed of similar samples. Based on these analyses, we suggest that having ~300 samples per dataset, ~200 shared known metabolites, and $r^2 > 0.4$ in terms of metabolite correlation similarity should be sufficient to achieve matching performance similar to what we describe in this paper. However, empirical assessment of matching performance using shared knowns is still recommended for new datasets.

Genetic validation of matched signals. After demonstrating that the matching method could be used to accurately pair up shared known metabolites, we next sought to validate the

full set of matches. Because there is no uniform "gold standard" for matching unknown signals, we used genetic data to validate matched signals between OE and MCDS, reasoning that useful matches would have similar patterns of genetic association across the two cohorts. We performed a GWAS in both OE and MCDS for the matched signal pairs (4,432 "multiple" matches, 1,573 of which were "reciprocal"); we also analyzed an additional 207 pairs of shared knowns and 20 sets of 4,432 randomly matched pairs to serve as positive and negative controls, respectively. To assess how well we had selected matching pairs, we determined the overall directional consistency of association for the best-associated single nucleotide polymorphisms (SNPs) with the matched signal pairs. Specifically, for each matched pair, we identified the SNP with the best *p*-value in a GWAS meta-analysis of OE and MCDS, and tested whether the same allele was associated with increased metabolite levels across the two studies. (To avoid biasing the subsequent assessment of directional consistency, we forced all SNPs to have the same direction of effect when calculating meta-analysis *p*-values; see Methods).

For the 94 pairs of shared knowns that had genome-wide significant ($p < 5 \times 10^{-8}$) SNPs in the meta-analysis, 66 pairs (70.2%; Fisher's $p = 1.56 \times 10^{-4}$) showed directional consistency; in comparison, 478 out of 672 (71.1%; Fisher's $p = 1.83 \times 10^{-28}$) "reciprocal" or 1,119 out of 1,772 (63.1%; Fisher's $p = 3.08 \times 10^{-28}$) "multiple" matched pairs were consistent, both of which were significantly better than randomly matched signals (average consistency of 52.1%; empirical $p < 0.05$; **Fig 2A–2C**). Importantly, at more stringent *p*-value thresholds, as many as 91.4% of the "reciprocal" matched pairs had directional consistency, compared to a ceiling of 90.3% for the shared knowns, indicating that these matches for unknown signals show similar consistency as shared known metabolites (**Fig 2C**). In addition, we estimated true positive rate for the matched signals by assuming that true matches would show same degree of consistency as the shared knowns, and found that the "multiple" setting generated more true positive matches overall (**Fig 2D**), albeit at a lower confidence level (maximum true positive rate of 83.0%; **Fig 2E**). In summary, the most stringent application of our method ("reciprocal" setting) identified ~7 times as many high-confidence matches compared to the shared knowns. The method can also be used to generate many more potential matches under more lenient settings (e.g. cross-method matching, **S7 Fig**).

Application to perform GWAS replication and meta-analysis. In order to directly assess how much power we gained from matching metabolite signals, we also performed GWAS replication analysis using OE and MCDS as the discovery and replication cohorts, respectively. Out of 14 shared knowns that had genome-wide significant associations in OE, 7 had nominally significant ($p < 0.05$) and directionally consistent associations in MCDS. In comparison, 156 "reciprocal" matched signal pairs had genome-wide significant hits in OE, 56 of which had replicated associations in MCDS. Furthermore, after meta-analyzing the two cohorts (this time taking direction of effect into account), we found 71 shared knowns and 512 matched signal pairs with genome-wide significant associations. Among the significant matched signal pairs, 93 (18.2%) contained potentially redundant signals as the measured known metabolites: 48 pairs directly contained known metabolites; 45 pairs had m/z matching adduct masses of the known metabolites recorded in the Human Metabolome Database (HMDB) [16]. However, the rest of the significant matched pairs (81.8%) may be capturing additional metabolites not identified in our datasets: 225 had m/z matching adducts of unmeasured HMDB metabolites and 194 had m/z values with no record in HMDB (which may be previously characterized metabolites that have not been documented in HMDB, such as xenobiotics foreign to the human body, or truly novel molecules that have yet to be characterized). Based on these numbers, we estimated that our method enabled the identification of ~6 times more metabolite signals with significant associations.

Application to identify BMI-associated signals. To further showcase the utility of signal matching, we also applied our method to identify metabolite signals associated with BMI in

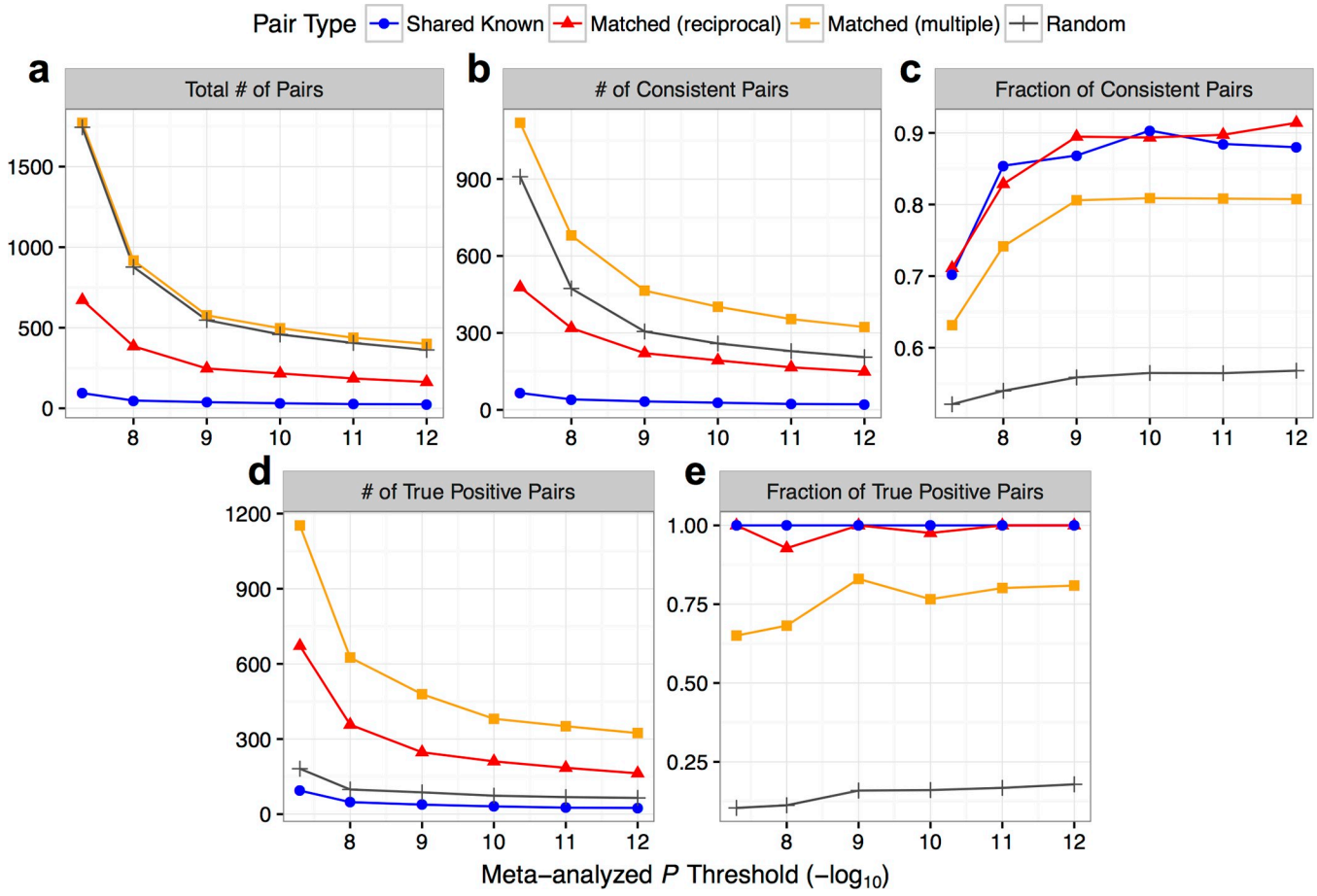

Fig 2. Genetic validation of OE-MCDS matched signals. GWAS were performed for "multiple" matched signal pairs (a subset of which were "reciprocal"), shared known pairs ("Shared Known", positive control), and randomly matched pairs (average statistics shown as "Random", negative control) in OE and MCDS, followed by meta-analysis that ignored direction of effect. For each pair, the SNP with the best meta-analyzed *p*-value was selected to assess directional consistency of its association in the two cohorts. (a) "Total # of Pairs": number of signal pairs with best SNPs below *p*-value threshold; (b) "# of Consistent Pairs" and (c) "Fraction of Consistent Pairs": number and fraction of pairs with directionally consistent best SNPs below *p*-value threshold; (d) "# of True Positive Pairs" and (e) "Fraction of True Positive Pairs": number and fraction of true positive pairs were estimated as described in Methods. X-axes start at genome-wide significant *p*-value threshold ($p < 5 \times 10^{-8}$). Error bars for "Random" pairs were excluded due to low visibility (all close to average).

https://doi.org/10.1371/journal.pcbi.1006734.g002

OE and MCDS. First, we identified 1,474 signals (114 known and 1,360 unknown) that were significantly ($p < 0.05/13,613$) associated with BMI in OE and tested for their replication in MCDS. Out of the 96 BMI-associated OE known metabolites that were also measured in MCDS, 75 (78.1%) showed directionally consistent association with BMI at a nominal significance threshold in MCDS (S3 Table). For BMI-associated OE signals that could not be compared directly in MCDS (i.e. unknowns or unshared knowns), we applied our matching procedure, and found 322 out of 425 (89.2%) "reciprocal" or 543 out of 790 (68.7%) "multiple" matched signal pairs to have directionally consistent and nominally significant association in MCDS (S3 Table). Again, by checking if these signal pairs contained known metabolites or had m/z matching adduct masses recorded in HMDB, we found 61 replicated "reciprocal" matched signal pairs to be potentially redundant with the measured known metabolites, 119 pairs to be related to HMDB metabolites not identified in our data, and 142 pairs with unrecorded m/z values. For replicated "multiple" matched signal pairs, 112 were related to measured knowns, 207 were related to other HMDB metabolites, and 224 were unrecorded in HMDB. Thus, by matching signals across OE and MCDS, we replicated 3.5–5.8 times more

BMI-associated signals compared to only looking at known metabolites identified in our datasets. Even if the unknown signals are not completely independent (i.e. multiple signals might correspond to one functional metabolite), the additional biological information extracted from the unknowns can be useful in pathway-based analyses that account for redundancy among signals, which we explored in the following section.

Generating pathway annotations for metabolite signals

Pathway method overview and calibration. Metabolic pathway annotations in public databases contain rich information for characterizing metabolites. However, these annotations are usually binary (i.e. a metabolite is either in or out of a pathway with no uncertainty) and only involve metabolites with known identities. Thus, in order to predict functions of unknown signals in our data and to perform well-powered pathway analysis, we developed an approach to assign metabolite signals to previously curated pathways (**Fig 1B**). First, we used profiling data from the BioAge cohort to construct "metabolic components" (MCs) that represent modules of covarying signals (**S8 Fig**). Next, we collected metabolic pathway annotations from ConsensusPathDB (CPDB) [17] and consolidated them into metabolite sets with unique metabolite combinations (i.e. one metabolite set may correspond to multiple pathways that contain identical sets of metabolites). We used the MCs to extend (reconstitute) the metabolite sets to include both known and unknown signals, resulting in a numeric signal-metabolite set annotation matrix, in which each signal was assigned a membership score in each set based on its similarity (across MCs) to metabolites originally curated to be in the set.

After reconstitution, we calculated a "label confidence score" to indicate how similar each reconstituted metabolite set is to the original pathways labeling the set; we also tested how well the reconstituted membership scores could be used to classify known metabolites into their original metabolite sets (see Methods). Using these performance measures, we calibrated different parameters in the reconstitution procedure (i.e. which metabolite sets and MCs to include) and picked the best-performing settings to construct the final BioAge annotation matrix (**S9 Fig** and **S4 Table**). Furthermore, to assess how sample size and number of known metabolites in the profiling dataset used for reconstitution would affect outcome, we carried out additional reconstitution analyses using random subsets of BioAge samples or known metabolites (**S10 Fig**). While we observed that larger sample size and known metabolite count both led to better reconstitution performance, increase in known metabolite count had a more dramatic influence compared to increase in sample size. When there was sufficient number of known metabolites in the dataset, relatively few samples were required to achieve good performance (**S10A Fig**).

Genetic validation of pathway annotations. We utilized OE genetic data to validate that the BioAge annotation matrix captures biologically relevant relationships. Specifically, we tested whether metabolite signals genetically associated with a gene would be enriched for reconstituted pathways related to that gene. First, we performed exome chip association analyses for all OE metabolite signals, mapped the signals with suggestive associations ($p < 1 \times 10^{-5}$) to BioAge using our matching procedure (in "multiple" setting), and derived a total of 6,465 associations between OE exome SNPs and BioAge matched signals. Next, we filtered the association results to select 36 loci that (1) contain coding SNPs associated with $> = 5$ signals and (2) contain genes curated to be in pathways reconstituted in the BioAge annotation matrix.

For each locus, we first used the BioAge annotation matrix to prioritize reconstituted metabolite sets enriched for the SNP-associated signals, and then checked whether the gene-related pathways showed up as enriched in the analysis. As negative control, we also repeated this procedure using 20 iterations of null association results. At an enrichment significance

Table 2. Top loci identified during genetic validation of BioAge pathway annotations.

Locus (SNP)	Chr	Alleles	Gene	Mutation	Associated signals*	Enriched pathways ($p < 0.01$) linked to gene
rs1105879	2	A/C	*UGT1A6*	R184S	1-methylnicotinamide, 54 unknowns	EHMN:Porphyrin metabolism; KEGG:Porphyrin and chlorophyll metabolism—Homo sapiens (human); Reactome:Metabolism of porphyrins
rs36004833	**7**	**A/G**	***SLC13A4***	**P451S**	**creatine, sarcosine, 7 unknowns**	**Reactome:SLC-mediated transmembrane transport; Reactome:Transport of glucose and other sugars, bile salts and organic acids, metal ions and amine compounds**
rs5030858	**12**	**C/T**	***PAH***	**R408W**	**phenylalanine, cholate, 10 unknowns**	**Reactome:Metabolism of amino acids and derivatives; Wikipathways: Biogenic Amine Synthesis; Wikipathways:SIDS Susceptibility Pathways; Reactome:Phenylalanine and tyrosine catabolism; SMPDB:Tyrosinemia Type 2 (or Richner-Hanhart syndrome); SMPDB:Phenylalanine and Tyrosine Metabolism; SMPDB:Phenylketonuria; SMPDB:Tyrosinemia Type 3 (TYRO3); KEGG:Phenylalanine, tyrosine and tryptophan biosynthesis—Homo sapiens (human); KEGG:Phenylalanine metabolism —Homo sapiens (human); HumanCyc:phenylalanine degradation/ tyrosine biosynthesis**
rs30842	16	T/G	*GOT2*	V346G	5 TAGs (C46:2, C46:3, C48:3, C48:4, C48:5), 6 unknowns	INOH:Glycine Serine metabolism; SMPDB:4-Hydroxybutyric Aciduria/ Succinic Semialdehyde Dehydrogenase Deficiency; SMPDB:Glutamate Metabolism; SMPDB:2-Hydroxyglutric Aciduria (D And L Form); SMPDB: Hyperinsulinism-Hyperammonemia Syndrome; SMPDB:Succinic semialdehyde dehydrogenase deficiency; SMPDB:Homocarnosinosis; INOH: Phenylalanine degradation; HumanCyc:4-hydroxyproline degradation; KEGG:Phenylalanine metabolism—Homo sapiens (human)
rs11657051	**17**	**C/T**	***ARSG***	**R398W**	**26 unknowns**	**Reactome:Gamma carboxylation, hypusine formation and arylsulfatase activation**

Bolded loci are discussed in main text. Pathway names are separated by ";".

* Unique BioAge signals matched to associated ($p < 1 \times 10^{-5}$) OE signals are shown.

https://doi.org/10.1371/journal.pcbi.1006734.t002

cutoff of $p < 0.01$, 5 out of 36 loci had gene-related enriched pathways (Table 2), compared to a mean of only 0.85 loci in null results (empirical $p < 0.05$; S5 Table). Even at less stringent enrichment significance thresholds, our approach performed better compared to null prioritization.

Examples of successful validation. We highlight three loci in which the enriched pathways have clear relevance to the affected genes' functions. First, SNP rs5030858 causes a missense mutation (R408W) in *PAH*, which encodes the phenylalanine hydroxylase responsible for converting phenylalanine to tyrosine, and the mutation is known to cause phenylketonuria [18]. In our analysis, the SNP was associated with phenylalanine, cholate, and 10 unknown signals. We performed m/z queries for the unknowns in HMDB and retrieved potential identities for 7 of the signals (S6 Table). In particular, one signal may be an adduct of phenylalanine (or a phenylalanine isomer); two others may be related to cinnamic acid and hypoxanthine, both of which have been linked to phenylalanine metabolism [19, 20]. On the other hand, 3 signals had no m/z record in HMDB and may be capturing metabolites that are underexplored in the human body, or even novel molecules that have not been characterized at all. The SNP-associated signals were enriched in 83 metabolite sets (corresponding to 129 pathways) at $p < 0.01$, with 8 of these sets containing pathways directly linked to *PAH* in CPDB (Table 2). Many other enriched sets are also related to phenylalanine and tyrosine metabolism, such as those involved in amine, neurotransmitter, and tryptophan metabolism (S7 Table).

Next, SNP rs36004833 is a missense variant (P451S) in *SLC13A4* and was associated with creatine, sarcosine, and 7 unknowns. HMDB m/z search showed that 3 of the unknowns may be adducts of creatine, 3 other signals matched (and thus may represent) adducts of creatinine, neohesperidin dihydrochalcone, and canavanine, and the last signal had no m/z record (S6

Table). However, we noted that the retention times for all of these unknowns (8.38–8.39 min) were close to that of creatine (8.38 min), thus they may have originated from creatine or other structurally similar metabolites. *SLC13A4* encodes a sodium/sulfate cotransporter that is known to be expressed in the high endothelial venules [21], and two of the metabolite sets enriched for the SNP-associated signals contain pathways linked to *SLC13A4* ("Reactome: SLC-mediated transmembrane transport" and "Reactome: Transport of glucose and other sugars, bile salts and organic acids, metal ions and amine compounds"; Table 2 and S8 Table). Importantly, the SNP-associated known metabolites, creatine and sarcosine, were not originally curated to be in these pathways in CPDB, thus the pathways could not have been detected without using our method.

Finally, SNP rs11657051 causes a missense mutation (R398W) in *ARSG* (Arylsulfatase G) [22] and was tentatively associated with 26 unknown signals (minimum $p < 1.72 \times 10^{-7}$). Most of the unknowns had no m/z record in HMDB, with only 4 signals potentially linked to chlorate, glutamine, and two metabolites found in cell membrane (a n-acyl pyrrolidine and a sphinogomyelin; S6 Table). However, upon closer inspection, we noted that except for the potential glutamine adduct (HILIC-pos_QI2842), the unknowns had similar retention times (7.64–7.65 min) and recurring m/z differences from each other, indicating that they may be potassium formate ion clusters formed as artifacts during the profiling procedure (S9 Table) [23]. Intriguingly, despite their likely non-biological nature, we were able to prioritize pathways directly or indirectly linked to *ARSG* using these SNP-associated unknowns (e.g. "Reactome: Gamma carboxylation, hypusine formation and arylsulfatase activation" and "Reactome: Heparan sulfate/heparin (HS-GAG) metabolism"; Table 2 and S10 Table), due to correlation between these unknowns and known metabolites. The tentative nature of the genetic associations and the likely artefactual nature of the unknowns mean that future validation of the correlations with known metabolites and additional investigation would be needed to understand whether and how this group of *ARSG*-associated unknowns was able to capture biologically relevant information related to *ARSG* activity.

Together, the genetic validation examples discussed in this section showcase how our approach can link both known and unknown metabolite signals to various biological pathways and functions. In some cases, unknown signals may serve as "proxies" that tag true biology even when they might not be biological and functional entities themselves.

Application to identify BMI-associated pathways. As a last demonstration of the utility of PAIRUP-MS, we applied both the signal matching and pathway annotation methods to identify metabolic pathways associated with BMI. First, we identified 1,474 and 1,289 signals associated with BMI in OE and MCDS, respectively (after correction for multiple testing), and matched the unshared signals from each cohort to a common reference cohort (BioAge) using the "multiple" match type setting. Between shared knowns and matched signals, we could map a total of 1,162 OE and 1,030 MCDS BMI-associated signals to BioAge. We performed separate pathway enrichment analyses using these two sets of signals and the BioAge reconstituted metabolite sets. In total, 218 (31.6%) and 179 (25.9%) out of 690 metabolite sets were enriched (FDR < = 5%) for the OE- and MCDS-matched signals, respectively (S11 Table). A total of 107 (15.5%) metabolite sets, corresponding to 215 pathways, were enriched in both analyses (overlap significance: Fisher's $p = 4.01 \times 10^{-20}$; Fig 3). These pathways are involved in a wide range of biological processes, including signal transduction, neurotransmission, synaptic function, macronutrient metabolism, immune system, and transport of various compounds.

To show that our methods increased power for detecting BMI-related pathways, we performed traditional overrepresentation analyses using only the BMI-associated known metabolites and the binary metabolite set annotations from CPDB, and found only 25 overrepresented sets for OE at 5% FDR, while MCDS had no significant sets at all (S12 Table).

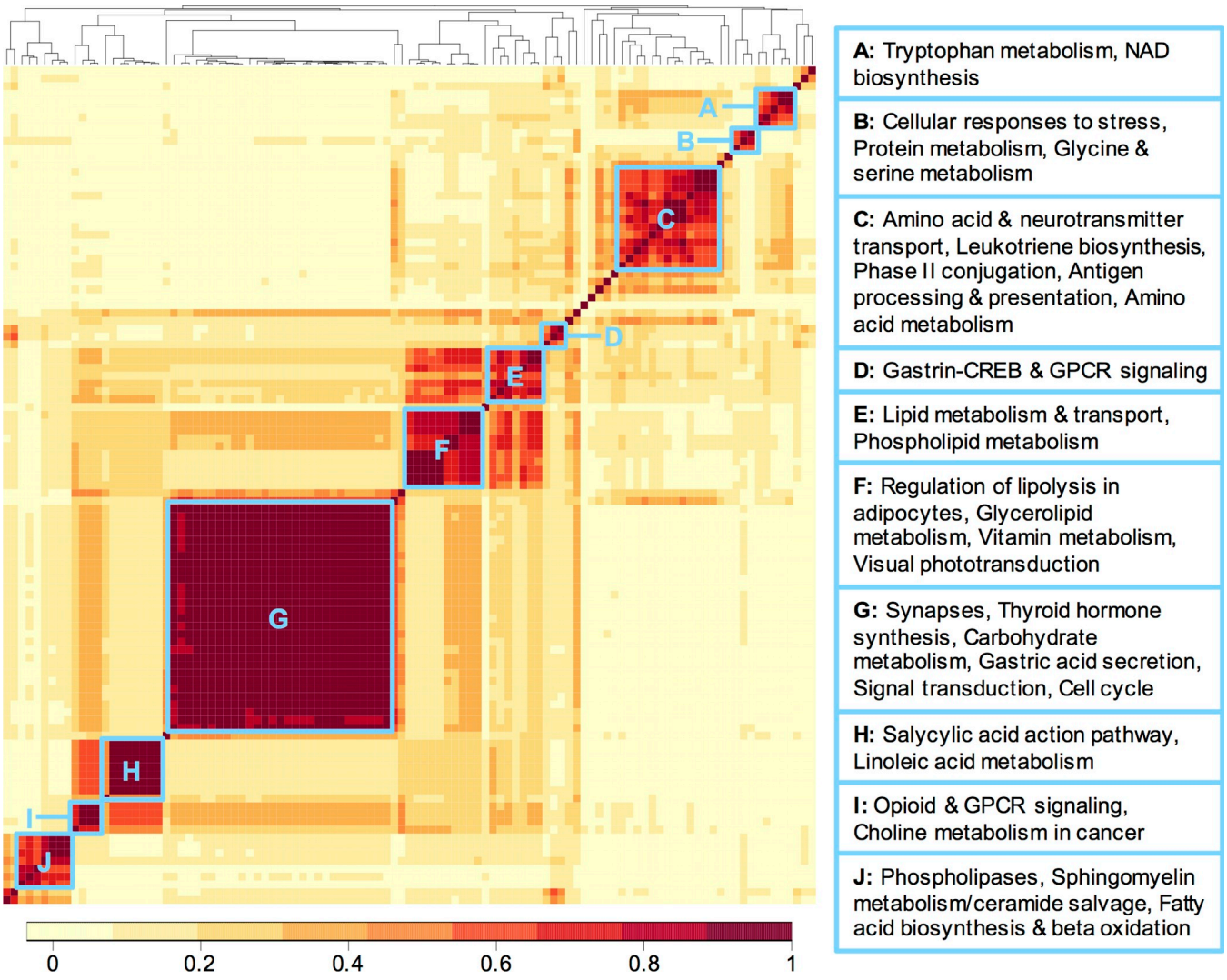

Fig 3. Clustered correlation heat map of 107 metabolite sets enriched (5% FDR) for both OE and MCDS BMI-associated signals. Correlation between metabolite sets were calculated using the BioAge annotation matrix. Color key indicates correlation values between each pair of metabolite sets. Distinct clusters (blue boxes with labels A-J) are highlighted, with representative pathway names in the clustered metabolite sets shown to the right of the heat map.

https://doi.org/10.1371/journal.pcbi.1006734.g003

These results demonstrate that PAIRUP-MS can be used to incorporate unknown signals into pathway-based analyses, thereby improving both power and interpretation in metabolomics studies.

Discussion

While untargeted profiling generates data for thousands of metabolite signals, most signals cannot be readily identified as known metabolites, are difficult to compare across studies, and consequently are often excluded from downstream analyses. In order to facilitate better use of untargeted data, we have developed PAIRUP-MS, an integrative tool for processing, matching, and annotating the unknown signals, which allowed us to compare them across MS-based datasets, extract useful information from their data, and improve power at detecting trait-associated biology. To our knowledge, no existing tools provide a similar streamlined and flexible framework for dealing with unknown signals across multiple datasets. Furthermore, unlike

previous methods designed to analyze unknown metabolites using specific biological variables (e.g. disease phenotype), PAIRUP-MS depends only on the metabolite profiling data to match and annotate the unknowns, before any additional data is required to perform downstream analyses.

Within PAIRUP-MS, we implemented a m/z and imputation-based method for matching unknown signals across datasets, demonstrated that it could be used to accurately pair up shared known metabolites, and showed that it could outperform a m/z and RT-based matching approach when RT information is unreliable. When we used genetic associations to validate a subset of the matched signals, we observed that the most stringent matches performed comparably in validation to the shared knowns. By including matched signals in combined association analyses (with genetic variants or with phenotypes), we were able to identify ~6 times more signals with significant replicated associations compared to the common practice of only studying known metabolites.

We also developed a pathway reconstitution procedure to annotate unknown signals using curated metabolic pathways. Again, we used genetic data to validate the pathway annotations, showing that signals associated with a gene were likely to be enriched for the gene-related pathways. Finally, we applied both the matching and pathway methods to identify BMI-associated pathways using a crossover approach (i.e. identifying trait-associated signals in one dataset but testing for enrichment using pathways built from another dataset), and demonstrated that it was more powerful than performing pathway overrepresentation analysis using only known metabolites.

Several study limitations and future directions should be considered. First, although the samples encompassed a range of ascertainments and were collected in different continents, all three datasets were generated by the same LC-MS profiling platform (albeit over different iterations of that platform). It will be valuable to test PAIRUP-MS using data from other platforms, as performance may be influenced by various technical differences between platforms (e.g. experimental setups of profiling assays, computational software used to detect signal peaks, types of metabolites measured and identified, etc.). The pathway method should be applicable to any profiling dataset that has sufficient number of samples and identified known metabolites, whereas the matching method is restricted to MS-based datasets with comparable metabolite correlation structures. We provide some guidelines for minimum requirements for using PAIRUP-MS, but calibrating parameters and assessing performance using known metabolites, as we have described in this study, will still be crucial to achieving good results when analyzing data from diverse studies and platforms.

Another study limitation concerns the fact that we only performed computational validation of PAIRUP-MS results in this paper. While our validation approaches enable systematic, unbiased assessment of results, they require genetic data to be available for the profiled samples. In particular, we could only validate OE-MCDS matched signals because BioAge genotypes were unavailable, and even the OE and MCDS cohorts had ancestry differences that complicated the interpretation of results (i.e. hard to determine if failed validation was due to false match or genetic difference). Larger numbers of untargeted profiling datasets with accompanying genetic data will allow the ongoing use of genetic data to assess the performance of PAIRUP-MS across a wider range of samples.

Experimental validation of the unknown signals is also an important future direction. Although PAIRUP-MS allows us to analyze unknown signals without knowing their chemical identities, individual signals of interest would ultimately have to be chemically characterized if we are to fully understand their biological functions. We performed m/z queries in HMDB to determine the potential identities of some unknown signals highlighted in this paper, but it is not possible to confirm these identities and distinguish between various adducts and isomers

without additional targeted profiling experiments. Moreover, as illustrated by the *ARSG* genetic validation example, even when unknown signals appear to be informative for biological inference, they may be non-biological entities that are correlated with functional metabolites. In this particular example, the likely artefactual nature of the unknowns means that independent confirmation of their correlations with known metabolites and with genetic variation in *ARSG* would be needed. If these correlations, especially with genetic variation at *ARSG*, were validated, it would raise the intriguing hypothesis that these non-biological entities may be an indirect readout of true biological variation across samples; in this case, further work would be required to identify the true biological connections.

Despite these caveats, by initially skipping over the bottleneck of metabolite identification, PAIRUP-MS offers a powerful way to prioritize unknown signals, so identification efforts can be focused on the unknowns that show the most robust biological or clinical significance across multiple cohorts. Furthermore, since the pathway annotation method in PAIRUP-MS can be used to classify unknown signals into previously defined metabolic pathways, it can provide an additional piece of information for deriving the identities of the unknowns. Once the identity of an unknown signal has been successfully validated, it can in turn be used as a known metabolite in new PAIRUP-MS analyses to improve functional prediction for the rest of the unknowns. In the future, experimental validation of unknown signals prioritized by PAIRUP-MS should be performed to assess how successfully PAIRUP-MS and metabolite identification can be used to complement each other in a synergistic manner.

The matching approach in PAIRUP-MS can also be combined with previous methods that have been developed around the concept of using biologically meaningful associations (e.g. with genetic variation or with disease phenotype) to prioritize unknown signals for follow-up investigation [10, 14, 15]. These methods were designed to be applied to one untargeted dataset at a time and thus may have power to detect only the very strongest associations. By harmonizing unknown signals across datasets using only the metabolite data itself (i.e. without using genetic or other phenotypic information), PAIRUP-MS can enhance the applications of these methods, allowing them to be used to analyze joint datasets of larger sample sizes, thus increasing the number of robust associations that can be detected between the unknowns and other genetic or phenotypic variables.

Finally, while we focused on analyzing pairs of datasets in this paper, large-scale meta-analysis requires a framework to match and compare many datasets simultaneously. Our current recommendation would be to define a "reference panel" dataset and match metabolite signals in all other datasets to this common reference (analogous to reference panels for genotype imputation). The choice of the reference panel could be made after assessing the performance of matching shared known metabolites across pairs of datasets. A reference dataset that incorporates diverse samples and captures a wide range of metabolite abundance variation would also be ideal for building reference pathway annotations that can be used to annotate all signals that are matched to the reference.

In conclusion, we have developed a suite of methods, PAIRUP-MS, for analyzing unknown signals in untargeted profiling data and showed that it can be applied to improve power and make biological inferences in metabolomics analyses. Matching across datasets is vital for increasing power through meta-analysis (e.g. imputation enabled meta-analysis of GWAS data across different genotyping platforms). Similarly, PAIRUP-MS can enable much more powerful analyses and meta-analyses of the great majority of untargeted metabolomics data that has not yet been systematically examined. The availability of many more untargeted datasets (especially with accompanying genetic data) will allow these analyses to be performed in much larger sample sizes and should also allow further refinement and evaluation of our methods across a wider range of datasets, samples, and platforms.

Methods

Metabolomics datasets and data processing

Obesity Extremes cohort (OE). Metabolite profiling was performed on plasma samples of 300 individuals from the Estonian Biobank of the Estonian Genome Center at the University of Tartu (EGCUT) [24]. The individuals were selected from the extremes of the BMI distribution to include 100 lean (BMI < 20), 100 obese (BMI > 34), and 100 random individuals matched for age, sex, and fasting time ($> = 4$ hr). Clinical data were examined to exclude any individuals with pregnancy, anorexia, or known wasting illnesses. Profiling was done using 4 LC-MS methods to measure 393 known metabolites and 18,667 unknown signals.

Mexico City Diabetes Study cohort (MCDS). Metabolite profiling was performed on fasting plasma samples collected from 865 individuals in the Mexico City Diabetes Study at the 1998 exam cycle. Details of this prospective cohort have been described previously [25]. 3 LC-MS methods were used to measure 306 known and 11,888 unknown signals.

BioAge Labs Mortality cohort (BioAge). Metabolite profiling was performed on plasma samples of 583 individuals 70–80 years old and free of major morbidity at enrollment, selected from the Estonian Biobank as a mortality cohort. None of the BioAge samples overlap with OE. 4 LC-MS methods were used to measure 629 known and 19,087 unknown signals.

Metabolite data processing. An overview of the data processing scheme is shown in **S1 Fig**. Starting with datasets in which signal peaks have been detected, aligned and quantified and where several hundred known metabolites have been identified, we performed the following steps on each dataset before using it in downstream analyses: (1) log-transformed and normalized the data using internal standards and interspersed pooled plasma samples, (2) removed outlier data points and signals with noisy variation trends, (3) removed samples and signals with $> 25\%$ (OE) or 50% (MCDS and BioAge) missing data, (4) imputed missing values using the MICE R package (v2.25) [26], (5) adjusted each signal for covariates if appropriate (only done for data used in genetic and BMI association analyses: age, sex, and fasting time for OE; age and sex for MCDS), and (6) performed rank-based inverse normal transformation to calculate abundance z-scores for each signal.

All participants in OE, MCDS, and BioAge provided informed consent. This study was approved by their respective local ethics committees and the Boston Children's Hospital Institutional Review Board. More details of the metabolite profiling, quality control, and missing value imputation procedures are described in **S1**–**S3 Text**.

Matching metabolite signals across datasets

Checking for m/z agreement. We implemented an algorithm to check whether the difference between 2 m/z values are within $d \pm 0.005$ of each other. While $d = 0$ in the most basic setting, it can be set to multiple values when taking ionization modes and adduct ions into account as shown in **S13 Table**. In particular, we implemented 2 settings: (1) "No adduct": only the most common positive or negative adduct ion (i.e. $[M+H]^+$ and $[M+H]^-$) is considered, or (2) "Adduct": multiple adduct ions are considered. (In this paper, we selected the ions used in "adduct" setting by observing m/z differences between shared known metabolites in our datasets: we included M^+, $[M+H]^+$, $[M+NH_4]^+$, and $[M+Na]^+$ for positive ionization mode and $[M-H]^-$ for negative ionization mode. However, additional or alternative adduct ions may be specified when running the algorithm to accommodate different types of datasets to test whether different sets of adducts improve matching performance.) When identifying all signal pairs with agreeing m/z values across two datasets, we also implemented a third "combined" setting, where the "adduct" setting was used only when the "no adduct" setting failed to

identify any pairs with matching m/z values. We tested all 3 settings in **Parameter calibration** to identify the optimal setting to use for matching signals across each pair of datasets.

Calculating imputation-based correlation. To impute a signal from Dataset 1 to Dataset 2, we fit a linear regression model for the signal using Dataset 1 data, which included all known metabolites shared by the two datasets as predictors, and then applied the resulting model to Dataset 2 data to predict the signal's abundance in Dataset 2 samples. The reversed process was done to impute signals from Dataset 2 to Dataset 1. When performing imputation for the shared knowns (used as positive controls in **Parameter calibration**), we built a leave-one-out model for each known metabolite *m*, where all shared knowns except for *m* were used as predictors. After imputation, we calculated pairwise correlation between Dataset 1 and Dataset 2 signals using 3 different settings: (1) "Dataset 1 correlation": correlate Dataset 1 (observed) and Dataset 2 (imputed) signals across Dataset 1 samples, (2) "Dataset 2 correlation": correlate Dataset 1 (imputed) and Dataset 2 (observed) signals across Dataset 2 samples, or (3) "All correlation": merge observed and imputed data and correlate signals across all samples. We evaluated these settings in **Parameter calibration** to identify the optimal approach to use for **Matching based on m/z and correlation**.

Matching based on m/z and correlation. In general, to match a Dataset 1 signal, *s*, to a Dataset 2 signal, we would first identify all Dataset 2 signals whose m/z agree with *s*, and then select the one that is best correlated with *s* to be the final match. If no Dataset 2 signals share matching m/z with *s*, then *s* is not matched at all. We implemented variations of this procedure and compared their performance in **Parameter calibration**. First, since the matching procedure is directional (i.e. matching from Dataset 1 to 2 vs. 2 to 1 could be different), we distinguished between 3 types of matches, each type being a subset of the previous type: (1) "Multiple": all matches that can be made as described by the general guideline above, which allows multiple-to-1 matching (i.e. multiple Dataset 1 signals can be mapped to the same Dataset 2 signal), (2) "Unique": unique 1-to-1 matches that only keep the best (in terms of correlation) Dataset 1 signal mapped to each Dataset 2 signal, or (3) "Reciprocal": unique, bidirectional 1-to-1 matches that appear both when matching from Dataset 1 to 2 and from 2 to 1. We also allowed 2 partition settings: (1) "Within method": only look for matches among signals measured using the same profiling method, or (2) "Across method": look for matches across datasets regardless of differences in profiling methods. Lastly, we implemented an optional correlation cutoff for calling matches (i.e. only keep matched pairs whose correlation is greater than the cutoff).

Matching based on m/z and RT. We implemented a crude RT-based matching procedure to serve as a comparison to our imputation-based method. Here, to match signals from Dataset 1 to Dataset 2, we would first use RTs of shared knowns to fit a linear model for predicting the RT shift between the two datasets. Then, to match a Dataset 1 signal, *s*, to a Dataset 2 signal, we would predict the RT of *s* in Dataset 2 using the fitted model, find all Dataset 2 signals whose m/z agree with *s*, and then select the one whose RT is closest to the predicted RT to be the final match. Just as we did for **Matching based on m/z and correlation**, we tested different match types ("multiple", "unique", or "reciprocal") and partition settings ("within method" or "across method") in **Parameter calibration**.

Parameter calibration. To calibrate all of the parameters described above (i.e. adduct ion setting, correlation setting, match type, partition setting, and correlation cutoff), we treated known metabolites shared across two datasets as unmatched signals and applied our procedures to match them up. For each pair of datasets (i.e. OE-MCDS, OE-BioAge, or MCDS-BioAge), we calculated the number and percentage of (1) correct matches: Dataset 1 metabolite is matched to itself in Dataset 2, (2) highly correlated matches: Dataset 1 metabolite is matched to a signal that is highly correlated ($r^2 > 0.8$) with itself in Dataset 2, and (3) incorrect but highly correlated matches: matches in (2) but not in (1).

GWAS and genetic validation of matched signals

GWAS and meta-analysis. 294 OE samples with Estonian reference imputed genotypes and 637 MCDS samples with 1000 Genomes phase 3 imputed genotypes were used to perform GWAS for the OE-MCDS shared known and matched signal pairs (see **S4 Text** for genotyping and imputation details). We used the linear mixed model and kinship matrix calculation methods in EPACTS (v3.2.6) [27] to analyze each cohort, restricting analyses to biallelic SNPs with minor allele count > = 3 in the cohort and including genotyping platform/backbone as a covariate. SNPs that overlap between the 2 cohorts were meta-analyzed using the inverse variance weighted method in METAL (2011-03-25 version) [28].

Validation analysis. For each pair of shared knowns or matched signals, we performed an alternative meta-analysis that ignored direction of effect (i.e. forcing all effect size estimates to be positive), identified the SNP with the best meta-analyzed *p*-value, and determined if its original effect size estimates in OE and MCDS were directionally consistent. We combined results for individual signal pairs to calculate the number and fraction of consistent pairs among shared knowns or matched signals at different *p*-value thresholds (i.e. only considering pairs whose best SNPs pass the threshold). We used Fisher's exact test to evaluate statistical significance of the observed degree of consistency. Additionally, for the matched signals, we performed 20 null permutations by shuffling the mapping between matches (i.e. generating randomly matched pairs), and then calculated an empirical *p*-value for the observed consistency fraction (i.e. p = proportion of null fractions greater than or equal to the observed fraction). Finally, we estimated the fraction of true positive pairs (i.e. true positive rate) at each *p*-value threshold to be: max[(c–0.5)/(s– 0.5), 1] where c = fraction of consistent pairs and s = fraction of consistent shared knowns, and then derived the number of true positive pairs using this fraction.

Generating pathway annotations for metabolite signals

Metabolic pathway and metabolite set annotations. We collected metabolic pathway annotations from CPDB (release 31) [17], which aggregated data from 11 source databases. We filtered the annotations to obtain pathways containing > = 2, 5, or 10 known metabolites profiled in BioAge and assigned a "*database*:*name*" label to each pathway, where *database* refers to the source database and *name* is the pathway name as shown in that database. We further consolidated the pathways into metabolite sets, with each set representing all pathways sharing the same metabolite combination, excluding metabolites not profiled in BioAge. The resulting metabolite set annotations were used as input data in **Signal-metabolite set annotation matrix**. CPDB also contains annotations that link genes to pathways based on previous literature evidence, which we utilized in **Genetic validation of pathway annotations**.

Metabolic components. We calculated pairwise Spearman correlation for all metabolite signals (known and unknown) across BioAge samples, and then performed principal component analysis on the correlation matrix to derive "metabolic components" (MCs; eigenvectors that represent modules of correlated signals) and a corresponding signal-MC score matrix. In order to assess if the MCs captured biological patterns contained within metabolite sets derived from CPDB, we performed enrichment analysis using the MC scores of known metabolites included in the metabolite sets. For each MC and each set, we performed a two-tailed Wilcoxon rank-sum test to compare the MC scores of metabolites in the set vs. other metabolites. We repeated the tests using 20 iterations of null, permuted MC scores and estimated the FDR for each observed rank-sum *p*-value threshold, P, to be: (average number of null *p*-values < = P per iteration) / (number of observed *p*-values < = P). This FDR was used to filter MCs as described in **Parameter calibration**.

Signal-metabolite set annotation matrix. We used the MC scores of metabolite signals to reconstitute the CPDB metabolite sets, adopting a previously described framework for gene

set reconstitution [29]. Again, we performed a two-tailed Wilcoxon rank-sum test to compare the MC scores of known metabolites in the set vs. not in the set for each metabolite set-MC pair, but this time storing the results as a metabolite set-MC matrix of rank-sum *z*-scores. Next, we used the signal-MC matrix (from **Metabolic components**) and the metabolite set-MC matrix to calculate the Spearman correlation between each signal-metabolite set pair across the MCs, resulting in a signal-metabolite set annotation matrix of correlation scores. To avoid overfitting, when calculating the matrix scores of a known metabolite originally annotated in a set, we repeated the reconstitution procedure by leaving out the data for this metabolite.

Parameter calibration. A calibration procedure was carried out to determine which metabolite sets and MCs to use for constructing the optimal signal annotation matrix. We tested metabolite sets containing $>=$ 2, 5, or 10 known metabolites profiled in BioAge. For MCs, we tested the top 50, 100, or 583 MCs (in terms of variance explained), or filtered for any MCs that were enriched for $>=$ 1 metabolite set at 1% or 5% FDR (see **Metabolic components**). After generating annotation matrices using different parameters, for each matrix, we converted correlation scores of known metabolites into *p*-values, and then evaluated how well these *p*-values could be used to classify metabolites into their original metabolite sets using a receiver operating characteristic (ROC) curve and area under the curve (AUC) approach. We also performed post-reconstitution enrichment analysis to identify reconstituted metabolite sets enriched for metabolites originally curated to be in the set (see **Metabolite set enrichment analysis**). The enrichment *p*-values from this analysis were used as "label confidence scores" for the metabolite sets.

Genetic validation of pathway annotations

Exome chip association analysis. A subset of 281 OE samples were genotyped using the Illumina HumanOmniExpressExome BeadChip (v1.2). We performed association analysis for each OE metabolite signal using this genetic dataset to identify exome SNPs associated with signal abundance. We restricted our analyses to 57,220 exome SNPs with minor allele count $>=$ 3 and call rate $>=$ 0.5 in OE, using the linear mixed model and kinship matrix calculation methods in EPACTS (v3.2.6) [27].

Validation analysis. We filtered the OE exome chip association results using OE-BioAge "multiple" matched signals to identify associations between OE SNPs and BioAge signals. We grouped the associations by SNPs and identified SNPs that (1) were associated with $>=$ 5 signals at $p < 1 \times 10^{-5}$, (2) cause missense or nonsense mutations in genes, and (3) affect genes linked to $>=$ 1 CPDB pathways used for reconstitution. If multiple SNPs were found for the same gene, we only kept the SNP with the best *p*-value. To perform validation analysis for each locus, we first used the BioAge signal annotation matrix to prioritize metabolite sets enriched for the SNP-associated signals (see **Metabolite set enrichment analysis**). Next, we determined if any pathways linked to the affected gene showed up as enriched across a range of enrichment *p*-value thresholds. For each threshold, we counted the number of loci for which $>=$ 1 gene-associated pathway was enriched, and then repeated the procedure using 20 iterations of null exome chip association results (i.e. identifying top signals associated with random genotypes) to generate null counts for comparison. We calculated the empirical *p*-value for the observed count to be the proportion of null counts $>=$ the observed count.

BMI-associated metabolite signals and metabolite sets

Metabolite signals. We calculated BMI *z*-scores for both OE and MCDS samples by adjusting raw BMI for age and sex and performing rank-based inverse normal transformation on the residuals. For OE, all samples in the Estonian Biobank were included during *z*-score calculation; for MCDS, only samples in the cohort were included. We performed linear

regression to test for association between BMI *z*-scores and signal abundance *z*-scores in both cohorts and identified BMI-associated signals at Bonferroni-corrected significance thresholds ($p < 0.05/13{,}613$ for OE; $p < 0.05/7{,}136$ for MCDS).

Metabolite sets. We identified BioAge shared knowns or "multiple" matched signals corresponding to the BMI-associated OE and MCDS signals from the previous section, and then used these signals and the BioAge signal annotation matrix to perform two separate enrichment analyses as described in **Metabolite set enrichment analysis**. After identifying enriched metabolite sets at 5% FDR in both analyses, we performed a Fisher's exact test to evaluate the statistical significance of the overlap.

Metabolite set enrichment analysis

A schematic overview of how we calculated statistical significance in metabolite set enrichment analysis is shown in S11 Fig.

Rank-sum *p*-value. To calculate the enrichment of each metabolite set in the signal annotation matrix given a "positive" and a "negative" list of signals, we used a two-tailed Wilcoxon rank-sum test to compare the metabolite set scores (absolute correlation) of the positive vs. negative signals to get a nominal *p*-value. For post-reconstitution enrichment analysis (in **Generating pathway annotations for metabolite signals**), the positive and negative lists consisted of known metabolites in an original CPDB metabolite set vs. not in the set, respectively. For identifying trait-associated metabolite sets, the lists consisted of signals significantly associated with the trait (SNP genotype in **Genetic validation of pathway annotations**; BMI in **BMI-associated metabolite signals and metabolite sets**) vs. all other signals (restricting to signals that could be matched across datasets).

Permutation *p*-value. For **Genetic validation of pathway annotations** and **BMI-associated metabolite signals and metabolite sets**, we generated null lists of signals ranked by their association with 1000 sets of permuted trait scores and repeated the rank-sum tests using the null lists (i.e. taking the top *N* signals in each null list to be the "positive" list, where *N* = the number of signals in the observed positive list). We used the null enrichment results to adjust the observed rank-sum *p*-values for metabolite set-specific biases, calculating a permutation *p*-value for each metabolite set to be the proportion of null rank-sum *p*-values < = the observed rank-sum *p*-value.

FDR. For **BMI-associated metabolite signals and metabolite sets**, we implemented another level of permutations to estimate analysis-wide FDR that accounts for multiple hypothesis testing across metabolite sets. We generated 20 additional null signal lists and calculated their corresponding rank-sum *p*-values. By comparing these new null rank-sum *p*-values against the 1000 sets of null rank-sum *p*-values computed previously, we calculated 20 sets of null permutation *p*-values. The FDR for an observed permutation *p*-value threshold, *P*, was then estimated as: (average number of null permutation *p*-values < = *P* per null set) / (number of observed permutation *p*-values < = *P*). Finally, we forced the final FDR estimates to be monotonic (i.e. FDR for smaller *p*-values had to be < = FDR for larger *p*-values) to smooth out random fluctuations in null iterations.

Metabolite set overrepresentation analysis

Binary metabolite set annotations from CPDB were used to perform overrepresentation analysis given a list of trait-associated known metabolites. For each metabolite set, we created a 2×2 contingency table that categorized known metabolites based on trait association and metabolite set membership and used it to calculate a one-sided Fisher's exact *p*-value. Null permutations were performed as described in **Metabolite set enrichment analysis** (except using Fisher's exact test instead of rank-sum test) to calculate permutation *p*-value and FDR.

LC-MS m/z queries in HMDB

In order to determine potential identities of unknown signals prioritized in either the matching or pathway results sections, we performed m/z queries using the "LC-MS Search" tool in HMDB [16]. All adduct types (under the appropriate positive or negative ionization mode) were considered. Molecular weight tolerance window was set to ± 1 ppm.

Supporting information

S1 Fig. Overview of PAIRUP-MS data processing scheme. Data processing steps performed externally by Broad Metabolomics Platform or using existing software package (i.e. MICE) are highlighted in blue. Steps performed separately on data generated from each profiling method vs. on merged dataset containing data from all profiling methods are indicated by red text. All components of PAIRUP-MS were designed to be run in a streamlined manner, but each component can also be used independently depending on the characteristics of different datasets and analysis needs (see source code and documentation on https://github.com/yuhanhsu/PAIRUP-MS for details on input and output data format at each step).
(PDF)

S2 Fig. Comparison of known metabolite correlation structure between datasets. Pairwise correlation between shared known metabolites were calculated within each dataset then compared across (a) OE vs. MCDS, (b) OE vs. BioAge, and (c) MCDS vs. BioAge. R-squared (Rsq) of the pairwise correlation values were calculated to assess overall similarity.
(PDF)

S3 Fig. OE-MCDS shared known matching calibration results. Matching was performed using different adduct ion (a), correlation (b), match type (c), partition (d), and correlation cutoff (x-axis) settings (see Methods for parameter explanations). In each panel, the parameters not being compared were set to the following default values: "Adduct", "All Correlation", "Reciprocal", and "Within Method". Dashed line in (b) shows optimal RT-based matching results for comparison. "Match Count": number of shared knowns matched; "Correct Fraction": fraction of correct matches; "Rsq0.8 Fraction": fraction of matches strongly correlated ($r^2 > 0.8$) with the correct known in observed data; "Incorrect Rsq0.8 Fraction": fraction of incorrect matches strongly correlated with the correct known.
(PDF)

S4 Fig. OE-BioAge shared known matching calibration results. Matching was performed using different adduct ion (a), correlation (b), match type (c), partition (d), and correlation cutoff (x-axis) settings (see Methods for parameter explanations). In each panel, the parameters not being compared were set to the following default values: "Combined", "Dataset1 Correlation", "Reciprocal", and "Within Method". Dashed line in (b) shows optimal RT-based matching results for comparison. "Match Count": number of shared knowns matched; "Correct Fraction": fraction of correct matches; "Rsq0.8 Fraction": fraction of matches strongly correlated ($r^2 > 0.8$) with the correct known in observed data; "Incorrect Rsq0.8 Fraction": fraction of incorrect matches strongly correlated with the correct known.
(PDF)

S5 Fig. MCDS-BioAge shared known matching calibration results. Matching was performed using different adduct ion (a), correlation (b), match type (c), partition (d), and correlation cutoff (x-axis) settings (see Methods for parameter explanations). In each panel, the parameters not being compared were set to the following default values: "Combined", "All Correlation", "Reciprocal", and "Within Method". Dashed line in (b) shows optimal RT-based

matching results for comparison. "Match Count": number of shared knowns matched; "Correct Fraction": fraction of correct matches; "Rsq0.8 Fraction": fraction of matches strongly correlated ($r^2 > 0.8$) with the correct known in observed data; "Incorrect Rsq0.8 Fraction": fraction of incorrect matches strongly correlated with the correct known.
(PDF)

S6 Fig. Shared known matching performance using data containing different number of samples and shared known metabolites. MCDS-BioAge matching was performed using (a) random subsets of MCDS and BioAge samples (and 217 shared known metabolites) or (b) random subsets of shared known metabolites (and 821 MCDS and 583 BioAge samples). For each matching analysis, the fraction of matched knowns that was correct ("Correct") or highly correlated ("Rsq > 0.8") with the correct match is plotted. In (a), "Number of Samples" indicates sample size per dataset; red and blue dashed lines indicate the correct and highly correlated fractions, respectively, when using all 821 MCDS and 583 BioAge samples to perform matching. Optimal MCDS-BioAge matching parameters shown in **S2A Table** were used for all analyses.
(PDF)

S7 Fig. Genetic validation of OE-MCDS cross-method matched signals. GWAS were performed for "multiple" matched signal pairs (a subset of which were "reciprocal"), shared known pairs ("Shared Known", positive control), and randomly matched pairs (average statistics shown as "Random", negative control) in OE and MCDS, followed by meta-analysis that ignored direction of effect. For each pair, the SNP with the best meta-analyzed *p*-value was selected to assess directional consistency of its association in the two cohorts. (a) "Total # of Pairs": number of signal pairs with best SNPs below *p*-value threshold; (b) "# of Consistent Pairs" and (c) "Fraction of Consistent Pairs": number and fraction of pairs with directionally consistent best SNPs below *p*-value threshold; (d) "# of True Positive Pairs" and (e) "Fraction of True Positive Pairs": number and fraction of true positive pairs were estimated as described in Methods. X-axes start at genome-wide significant *p*-value threshold ($p < 5 \times 10^{-8}$). Error bars for "Random" pairs were excluded due to low visibility (all close to average).
(PDF)

S8 Fig. Characteristics of the BioAge metabolic components (MCs). Principal component analysis was performed on the BioAge metabolite signal correlation matrix to derive the MCs. (a) Cumulative variance explained (left y-axis) or Cronbach's alpha (right y-axis) of the MCs. (b) Number of CPDB metabolite sets that were enriched for each MC at 5% FDR.
(PDF)

S9 Fig. Calibration statistics for BioAge signal-metabolite set annotation matrix. Annotation matrices generated using different combinations of (a) metabolite sets and (b) MCs were used to classify known metabolites into their original metabolite sets, generating a ROC curve (with corresponding area under the curve, AUC) for each matrix (see Methods for details). (c) We also compared an annotation matrix containing only the confidently reconstituted metabolite sets (i.e. label confidence score < 0.05; "Filtered") against the full matrix ("Unfiltered"). In each panel, the parameters not being compared were set to the following default values: "Metabolites = 2" (i.e. metabolite sets containing > = 2 metabolites), "MCs = fdr0.05" (i.e. MCs enriched for > = 1 metabolite set at 5% FDR), and "Filtered". "Null" statistics were calculated using permuted annotation matrix.
(PDF)

S10 Fig. Metabolite set reconstitution performance using data containing different number of samples and known metabolites. BioAge signal-metabolite set annotation matrices

were generated using (a) random subsets of BioAge samples (and 603 known metabolites) or (b) random subsets of known metabolites (and 583 samples). For each resulting annotation matrix, the area under the curve (AUC) and the number or fraction of confidently reconstituted metabolite sets (i.e. label confidence score < 0.05) are plotted (see Methods for description of statistics). Metabolites sets containing $> = 2$ known metabolites and the top N MCs (N = sample size) were included for reconstitution in each analysis.
(PDF)

S11 Fig. Calculating statistical significance in metabolite set enrichment analysis. (a) Rank-sum *p*-value: Metabolite signals were split into positive (hatched pattern) and negative lists based on association with a variable of interest (e.g. BMI). The lists were used to perform two-tailed Wilcoxon rank-sum test to calculate observed (obs.) rank-sum *p*-value for each metabolite set. 2 rounds of null permutations (i.e. associating signals with randomly permuted variable) were used to calculate null rank-sum *p*-values. (b) Permutation *p*-value: Observed permutation (perm.) *p*-value for each metabolite set was calculated by comparing the observed rank-sum *p*-value against 1000 sets of null rank-sum *p*-values (from permutation round 1); 20 sets of null permutation p-values were calculated by comparing 20 sets of null rank-sum *p*-values (from permutation round 2) against another 1000 sets of rank-sum *p*-values (from permutation round 1). (c) FDR: The analysis-wide FDR for an observed permutation *p*-value threshold, *P*, was estimated by comparing the observed permutation *p*-values against the 20 sets of null permutation *p*-values.
(PDF)

S1 Table. Known metabolites included in QC'ed OE, MCDS, and BioAge metabolite data. "NA": m/z and RT information not available.
(XLSX)

S2 Table. (a) Optimal parameter settings and corresponding calibration statistics for matching each pair of datasets. (b) Optimal parameter settings and corresponding calibration statistics for cross-method matching.
(PDF)

S3 Table. BMI association results for OE-MCDS metabolite signal pairs. Metabolite signals with profiling methods (HILIC-pos, C8-pos, or LIPID) as prefix in their names are unknowns. Lipid name abbreviations: CE (Cholesteryl ester), DAG (Diacylglycerol), TAG (Triacylglycerol), LPC (Lysophosphatidylcholine), LPE (Lysophosphatidylethanolamine), PC (Phosphtatidylcholine), PE (Phosphtatidylethanolamine), PI (Phosphtatidylinositol), PS (Phosphtatidylserine), SM (Sphingomyelin). Other metabolite name abbreviations: ADMA (Asymmetric dimethylarginine), NMMA (N-Monomethyl-L-arginine), SDMA (Symmetric dimethylarginine).
(XLSX)

S4 Table. Calibration statistics for BioAge signal-metabolite set annotation matrix.
(PDF)

S5 Table. Summary of genetic validation of BioAge pathway annotations.
(PDF)

S6 Table. Potential identities of unknown signals associated with rs5030858 (*PAH*), rs36004833 (*SLC13A4*), or rs11657051 (*ARSG*) loci. "Potential identity", "Chemical formula", "Adduct", and "HMDB ID" information was retrieved by performing m/z query in HMDB (see Methods).
(XLSX)

S7 Table. Metabolite set enrichment results for signals associated with rs5030858 (*PAH*) locus. "SET_ID": unique identifier assigned to each metabolite set; "Nominal_P": rank-sum *p*-value; "Perm_P": permutation *p*-value; "FDR": false discovery rate of the permutation *p*-value; "Label_P": label confidence score for the reconstituted metabolite set; "CPDB_Pathways": labels for the original pathways from CPDB, individual pathways are separated by '|'.
(XLSX)

S8 Table. Metabolite set enrichment results for signals associated with rs36004833 (*SLC13A4*) locus. "SET_ID": unique identifier assigned to each metabolite set; "Nominal_P": rank-sum *p*-value; "Perm_P": permutation *p*-value; "FDR": false discovery rate of the permutation *p*-value; "Label_P": label confidence score for the reconstituted metabolite set; "CPDB_Pathways": labels for the original pathways from CPDB, individual pathways are separated by '|'.
(XLSX)

S9 Table. Pairwise difference between m/z of signals associated with rs11657051 (*ARSG*) locus (except HILIC-pos_QI2842).
(XLSX)

S10 Table. Metabolite set enrichment results for signals associated with rs11657051 (*ARSG*) locus. "SET_ID": unique identifier assigned to each metabolite set; "Nominal_P": rank-sum *p*-value; "Perm_P": permutation *p*-value; "FDR": false discovery rate of the permutation *p*-value; "Label_P": label confidence score for the reconstituted metabolite set; "CPDB_Pathways": labels for the original pathways from CPDB, individual pathways are separated by '|'.
(XLSX)

S11 Table. Metabolite set enrichment results for BMI-associated signals in OE or MCDS. "SET_ID": unique identifier assigned to each metabolite set; "OE_Perm_P" or "MCDS_Perm_P": permutation *p*-value; "OE_FDR" or "MCDS_FDR": false discovery rate of the permutation *p*-value; "Label_P": label confidence score for the reconstituted metabolite set; "CPDB_Pathways": labels for the original pathways from CPDB, individual pathways are separated by '|'.
(XLSX)

S12 Table. Metabolite set overrepresentation results for BMI-associated known metabolites in OE or MCDS. "SET_ID": unique identifier assigned to each metabolite set; "OE_Perm_P" or "MCDS_Perm_P": permutation *p*-value; "OE_FDR" or "MCDS_FDR": false discovery rate of the permutation *p*-value; "CPDB_Pathways": labels for the original pathways from CPDB, individual pathways are separated by '|'.
(XLSX)

S13 Table. (a) Rules for checking for m/z agreement between 2 ions. (b) m/z values of different adduct ions included in "adduct" settings.
(PDF)

S1 Text. Details of metabolite profiling.
(PDF)

S2 Text. Details of quality control (QC) of metabolite data.
(PDF)

S3 Text. Details of missing value imputation for metabolite data.
(PDF)

S4 Text. Details of imputed genotype data.
(PDF)

Acknowledgments

We thank C. Astley, C. Clish, A. Ganna, A. Kamburov, R. Salem, and S. Vedantam for discussions on study design and/or methodology. We thank the Broad Metabolomics Platform and SIGMA T2D Consortium for sharing data resources.

Author Contributions

Conceptualization: Yu-Han H. Hsu, Tonu Esko, Joel N. Hirschhorn.

Formal analysis: Yu-Han H. Hsu, Tonu Esko.

Funding acquisition: Yu-Han H. Hsu, Andres Metspalu, Krista Fischer, Kristen Fortney, Eric K. Morgen, Tonu Esko, Joel N. Hirschhorn.

Methodology: Yu-Han H. Hsu, Claire Churchhouse, Tune H. Pers, Joel N. Hirschhorn.

Resources: Josep M. Mercader, Andres Metspalu, Krista Fischer, Kristen Fortney, Eric K. Morgen, Clicerio Gonzalez, Maria E. Gonzalez, Tonu Esko.

Software: Yu-Han H. Hsu, Claire Churchhouse.

Supervision: Joel N. Hirschhorn.

Visualization: Yu-Han H. Hsu.

Writing – original draft: Yu-Han H. Hsu, Joel N. Hirschhorn.

Writing – review & editing: Claire Churchhouse, Tune H. Pers, Josep M. Mercader, Eric K. Morgen, Tonu Esko.

References

1. Patti GJ, Yanes O, Siuzdak G. Innovation: Metabolomics: the apogee of the omics trilogy. Nat Rev Mol Cell Biol. 2012; 13(4):263–9. https://doi.org/10.1038/nrm3314 PMID: 22436749; PubMed Central PMCID: PMC3682684.
2. Suhre K, Gieger C. Genetic variation in metabolic phenotypes: study designs and applications. Nat Rev Genet. 2012; 13(11):759–69. https://doi.org/10.1038/nrg3314 PMID: 23032255.
3. Cheng S, Rhee EP, Larson MG, Lewis GD, McCabe EL, Shen D, et al. Metabolite profiling identifies pathways associated with metabolic risk in humans. Circulation. 2012; 125(18):2222–31. https://doi.org/10.1161/CIRCULATIONAHA.111.067827 PMID: 22496159; PubMed Central PMCID: PMC3376658.
4. Wang TJ, Larson MG, Vasan RS, Cheng S, Rhee EP, McCabe E, et al. Metabolite profiles and the risk of developing diabetes. Nat Med. 2011; 17(4):448–53. https://doi.org/10.1038/nm.2307 PMID: 21423183; PubMed Central PMCID: PMC3126616.
5. Fischer K, Kettunen J, Wurtz P, Haller T, Havulinna AS, Kangas AJ, et al. Biomarker profiling by nuclear magnetic resonance spectroscopy for the prediction of all-cause mortality: an observational study of 17,345 persons. PLoS Med. 2014; 11(2):e1001606. https://doi.org/10.1371/journal.pmed.1001606 PMID: 24586121; PubMed Central PMCID: PMC3934819.
6. Illig T, Gieger C, Zhai G, Romisch-Margl W, Wang-Sattler R, Prehn C, et al. A genome-wide perspective of genetic variation in human metabolism. Nat Genet. 2010; 42(2):137–41. https://doi.org/10.1038/ng.507 PMID: 20037589; PubMed Central PMCID: PMC3773904.
7. Kettunen J, Tukiainen T, Sarin AP, Ortega-Alonso A, Tikkanen E, Lyytikainen LP, et al. Genome-wide association study identifies multiple loci influencing human serum metabolite levels. Nat Genet. 2012; 44(3):269–76. https://doi.org/10.1038/ng.1073 PMID: 22286219; PubMed Central PMCID: PMC3605033.

8. Rhee EP, Ho JE, Chen MH, Shen D, Cheng S, Larson MG, et al. A genome-wide association study of the human metabolome in a community-based cohort. Cell Metab. 2013; 18(1):130–43. https://doi.org/10.1016/j.cmet.2013.06.013 PMID: 23823483; PubMed Central PMCID: PMC3973158.
9. Shin SY, Fauman EB, Petersen AK, Krumsiek J, Santos R, Huang J, et al. An atlas of genetic influences on human blood metabolites. Nat Genet. 2014; 46(6):543–50. https://doi.org/10.1038/ng.2982 PMID: 24816252; PubMed Central PMCID: PMC4064254.
10. Krumsiek J, Suhre K, Evans AM, Mitchell MW, Mohney RP, Milburn MV, et al. Mining the unknown: a systems approach to metabolite identification combining genetic and metabolic information. PLoS Genet. 2012; 8(10):e1003005. https://doi.org/10.1371/journal.pgen.1003005 PMID: 23093944; PubMed Central PMCID: PMC3475673.
11. Smith CA, Want EJ, O'Maille G, Abagyan R, Siuzdak G. XCMS: processing mass spectrometry data for metabolite profiling using nonlinear peak alignment, matching, and identification. Anal Chem. 2006; 78 (3):779–87. https://doi.org/10.1021/ac051437y PMID: 16448051.
12. Lommen A. MetAlign: interface-driven, versatile metabolomics tool for hyphenated full-scan mass spectrometry data preprocessing. Anal Chem. 2009; 81(8):3079–86. https://doi.org/10.1021/ac900036d PMID: 19301908.
13. Patti GJ, Tautenhahn R, Siuzdak G. Meta-analysis of untargeted metabolomic data from multiple profiling experiments. Nat Protoc. 2012; 7(3):508–16. https://doi.org/10.1038/nprot.2011.454 PMID: 22343432; PubMed Central PMCID: PMC3683249.
14. Li S, Park Y, Duraisingham S, Strobel FH, Khan N, Soltow QA, et al. Predicting network activity from high throughput metabolomics. PLoS Comput Biol. 2013; 9(7):e1003123. https://doi.org/10.1371/journal.pcbi.1003123 PMID: 23861661; PubMed Central PMCID: PMC3701697.
15. Pirhaji L, Milani P, Leidl M, Curran T, Avila-Pacheco J, Clish CB, et al. Revealing disease-associated pathways by network integration of untargeted metabolomics. Nat Methods. 2016; 13(9):770–6. https://doi.org/10.1038/nmeth.3940 PMID: 27479327; PubMed Central PMCID: PMC5209295.
16. Wishart DS, Feunang YD, Marcu A, Guo AC, Liang K, Vazquez-Fresno R, et al. HMDB 4.0: the human metabolome database for 2018. Nucleic Acids Res. 2018; 46(D1):D608–D17. https://doi.org/10.1093/nar/gkx1089 PMID: 29140435; PubMed Central PMCID: PMC5753273.
17. Kamburov A, Stelzl U, Lehrach H, Herwig R. The ConsensusPathDB interaction database: 2013 update. Nucleic Acids Res. 2013; 41(Database issue):D793–800. https://doi.org/10.1093/nar/gks1055 PMID: 23143270; PubMed Central PMCID: PMC3531102.
18. Gersting SW, Kemter KF, Staudigl M, Messing DD, Danecka MK, Lagler FB, et al. Loss of function in phenylketonuria is caused by impaired molecular motions and conformational instability. Am J Hum Genet. 2008; 83(1):5–17. https://doi.org/10.1016/j.ajhg.2008.05.013 PMID: 18538294; PubMed Central PMCID: PMC2443833.
19. Sarkissian CN, Gamez A. Phenylalanine ammonia lyase, enzyme substitution therapy for phenylketonuria, where are we now? Mol Genet Metab. 2005; 86 Suppl 1:S22–6. https://doi.org/10.1016/j.ymgme.2005.06.016 PMID: 16165390.
20. Ishimitsu S, Fujimoto S, Ohara A. Hydroxylation of phenylalanine by the hypoxanthine-xanthine oxidase system. Chem Pharm Bull (Tokyo). 1984; 32(11):4645–9. PMID: 6549439.
21. Girard JP, Baekkevold ES, Feliu J, Brandtzaeg P, Amalric F. Molecular cloning and functional analysis of SUT-1, a sulfate transporter from human high endothelial venules. Proc Natl Acad Sci U S A. 1999; 96(22):12772–7. PMID: 10535998; PubMed Central PMCID: PMC23093.
22. Ferrante P, Messali S, Meroni G, Ballabio A. Molecular and biochemical characterisation of a novel sulphatase gene: Arylsulfatase G (ARSG). Eur J Hum Genet. 2002; 10(12):813–8. https://doi.org/10.1038/sj.ejhg.5200887 PMID: 12461688.
23. Barri T, Dragsted LO. UPLC-ESI-QTOF/MS and multivariate data analysis for blood plasma and serum metabolomics: effect of experimental artefacts and anticoagulant. Anal Chim Acta. 2013; 768:118–28. Epub 2013/03/12. https://doi.org/10.1016/j.aca.2013.01.015 PMID: 23473258.
24. Leitsalu L, Haller T, Esko T, Tammesoo ML, Alavere H, Snieder H, et al. Cohort Profile: Estonian Biobank of the Estonian Genome Center, University of Tartu. Int J Epidemiol. 2015; 44(4):1137–47. https://doi.org/10.1093/ije/dyt268 PMID: 24518929.
25. SIGMA T2D Consortium, Williams AL, Jacobs SB, Moreno-Macias H, Huerta-Chagoya A, Churchhouse C, et al. Sequence variants in SLC16A11 are a common risk factor for type 2 diabetes in Mexico. Nature. 2014; 506(7486):97–101. https://doi.org/10.1038/nature12828 PMID: 24390345; PubMed Central PMCID: PMC4127086.
26. van Buuren S, Groothuis-Oudshoorn K. mice: Multivariate Imputation by Chained Equations in R. Journal of Statistical Software. 2011; 45(3):1–67. https://doi.org/10.18637/jss.v045.i03
27. Kang HM. EPACTS (Efficient and Parallelizable Association Container Toolbox).

28. Willer CJ, Li Y, Abecasis GR. METAL: fast and efficient meta-analysis of genomewide association scans. Bioinformatics. 2010; 26(17):2190–1. https://doi.org/10.1093/bioinformatics/btq340 PMID: 20616382; PubMed Central PMCID: PMC2922887.

29. Pers TH, Karjalainen JM, Chan Y, Westra HJ, Wood AR, Yang J, et al. Biological interpretation of genome-wide association studies using predicted gene functions. Nat Commun. 2015; 6:5890. https://doi.org/10.1038/ncomms6890 PMID: 25597830; PubMed Central PMCID: PMC4420238.